Title
NMR STUDIES OF CLUSTERING IN SOLIDS

Authors
Baum, J.
Pines, A.

Publication Date
1985-12-01

Lawrence Berkeley Laboratory
UNIVERSITY OF CALIFORNIA

Materials & Molecular Research Division

Submitted to Journal of the
American Chemical Society

NMR STUDIES OF CLUSTERING IN SOLIDS

J. Baum and A. Pines

December 1985

Prepared for the U.S. Department of Energy under Contract DE-AC03-76SF00098

DISCLAIMER

LBL-20922

NMR STUDIES OF CLUSTERING IN SOLIDS

J. Baum[+] and A. Pines

Department of Chemistry, University of California, Berkeley and

Materials and Molecular Research Division, Lawrence Berkeley Laboratory,

Berkeley, CA 94720.

[+]Present address: Department of Inorganic Chemistry, Oxford, England.

Abstract

We present a time-resolved multiple-quantum NMR experiment which allows us to determine the spatial distribution of atoms in materials lacking long-range order; in particular, we study the size and extent of atomic clustering in these materials. Multiple quantum NMR is sensitive to the distribution of spins in a solid. At the two extremes, uniformly distributed spins absorb rf quanta continuously whereas clustered groups of N spins can absorb only up to N quanta. Model experiments are demonstrated on the hydrogen distribution in selectively deuterated organic solids and in hydrogenated amorphous silicon.

Introduction

In this paper, we describe the application of nuclear magnetic resonance to the question of clustering in materials lacking long-range order. In such materials, standard methods of structural characterization, such as x-ray crystallography, are not useful. Examples of such disordered materials range from minerals, semiconductors, polymers and liquid crystals, to species adsorbed on surfaces and in zeolites. These materials often display important physical or electrical properties; for example, a critical level of hydrogen incorporation into amorphous silicon renders it a semiconductor used in many industrial applications.[1]

As an example of the type of problem we face in these disordered solids, figure 1 illustrates two extreme, possible, atomic configurations: in the first, the atoms are distributed randomly but uniformly within the sample, and in the second they are grouped together, forming clusters. Usually, an NMR spectrum of a solid will not reveal the basic difference between these two situations. In both cases, the spectrum will normally be broad and featureless; the linewidth, due primarily to the dipolar couplings between spins, does not contain sufficient information to establish any statistical information on the atomic distribution.

In contrast, by capitalizing on the dipolar couplings in a different manner, a time-resolved multiple quantum NMR experiment can be used to address the question of atomic distribution in such materials.[2,3] For example, if the uniformly distributed material is irradiated with rf quanta in an NMR experiment, it might be expected to absorb them continuously whereas, isolated clusters will absorb only a finite number.[4] In this paper, we show that indeed a time resolved multiple-quantum experiment,

whose statistics are very sensitive to atomic distributions, can be used to probe the nature and extent of clustering in solids. Model systems containing a variety of hydrogen atom distributions are investigated: in particular, totally isolated clusters, various concentrations of clusters ranging from dilute to fairly dense, and uniformly distributed environments are all studied. We illustrate how these different distributions affect the multiple quantum dynamics and how the tendency to clustering and information on cluster sizes can be determined from the time dependence of the multiple quantum intensities.

Time development of multiple-quantum coherences

In multiple quantum NMR individual spins become correlated with one another over time, through their dipolar couplings.[5] In this way, the usual Zeeman selection rule can be overcome and "forbidden transitions", where the difference in magnetic quantum number ΔM is equal to $0,\pm1,\pm2,..,\pm N$, can be excited. When $\Delta M=N$, N spins "flip" collectively from the ground state to the highest excited state. Experimentally, such multiple quantum coherences are formed by applying an appropriate radio-frequency pulse sequence to the system for a time τ, thereby creating a Hamiltonian which forces the spins to act collectively or in a group. For spins to become correlated, the system must evolve under this Hamiltonain for a time τ roughly proportional to the inverse of the pairwise dipolar interactions. Because the magnitude of the dipolar interaction is inversely proportional to the cube of the distance between two spins i and j,

$$D_{ij} \sim \frac{1}{r_{ij}^3} P_2(\cos \theta_{ij}), \quad (1)$$

two spins which are far apart require more time to communicate with one another than spins which are closer together. Therefore the rate at which multiple quantum coherences develop is determined by the dipolar coupling distributions present in the system. Because the spatial arrangements of atoms are reflected by the magnitude of the dipolar couplings, a time dependent multiple quantum experiment can yield information concerning the distribution of spins in a material.

Monitoring the time development of the multiple quantum coherences in an infinte spin system reveals that correlations develop between spins in a monotonic fashion. As time progresses, more spins can absorb more quanta of radiation and very high multiple quantum orders can be detected, experimentally in excess of 100.[2,6] However, if clusters of spins exist, then the time development of the multiple quantum coherences will be interrupted; the number of interacting spins will be limited, to a large extent, by the size of the cluster. Shown in figure 2 are ^1H multiple-quantum spectra for a polycrystalline sample (shown in the inset) in which hydrogen atom clusters of different molecules are effectively isolated from one another owing to the large perchlorinated cyclopentadiene rings. For this model clustered material, the appearance of the multiple-quantum spectra remain very similar up to preparation times of 300 μsec, after which many high multiple-quantum orders begin to develop. These higher orders are attributed to inter-molecular interactions. This material will be adressed in more detail in a later section.

Schematically, the inter-spin correlations which occur during the development of multiple-quantum coherences are represented in figure 3. If

a solid is composed of a uniform distribution of atoms, where the dipolar couplings between spins may be roughly comparable, then the time development will be expected to look like the one depicted in Figure 3a. As the uniformly distributed spins absorb more and more quanta of radiation, the spins become correlated with one another in a continuous manner. Over time, the number of communicating spins is essentially unbounded. And, the effective "size" of the system grows monotonically. However, if a solid contains isolated clusters, then the variation between inter and intra cluster dipolar couplings is large enough to preclude inter-cluster correlations on the experimental time scale. Consequently, as shown in Figure 3b after an initial induction period, during which multiple quantum coherences develop between spins with large dipolar couplings, the number of correlated spins will be expected to remain roughly constant over time and will reflect the size of the isolated cluster. If this group is truly independent of any other groups, then no additional interactons can build up on the experimental time scale. On the other hand, if small but non-negligeable dipolar couplings do exist between spins of different groups, then with time, the groups will communicate with one another. If the concentration of clusters is high, less time will be needed for intergroup communication to occur. Ultimately, for very long times, a large network of correlated spins will develop.

Experimental Methods

Multiple quantum NMR in solids has been described in detail elsewhere and we outline here only the salient points relevant to this work.[2,6] The two-dimensional multiple quantum experiment is divided into four periods each characterized by a time variable: preparation (τ), evolution (t_1),

mixing (τ), and detection (t_2).[7] The pulse sequence design is shown in figure 4. The radiofrequency pulse cycle of the preparation period is composed of eight $\pi/2$ pulses of length t_p separated by delays Δ and $\Delta' = 2\Delta + t_p$. The phases of the first and last four pulses are 0° and 180°, respectively. The total preparation period (τ) is created by repeating the 60 μsec basic cycle m times. This combination of pulses and delays creates a two-quantum average Hamiltonian,

$$\bar{H} = 1/3(H_{yy} - H_{xx}) = -1/2 \sum_{i<j} D_{ij}(I_{i+}I_{j+} - I_{i-}I_{j-}), \qquad (2)$$

where I_+ and I_- are raising and lowering angular momentum operators. This Hamiltonian allows multiple quantum coherence of even order to develop.[8] In addition, different multiple-quantum orders are separated from one another by using the method of time proportional phase incrementation.[9] Here, the preparation period pulses are phase shifted by ϕ for each value of t_1.

Following the preparation period, groups of coherently excited spins evolve in the presence of local dipolar fields for a time t_1. During the mixing period, the multiple quantum coherences are converted into observable single quantum coherences. In solids, a time reversed mixing period is necessary to ensure that individual overlapping lines within a multiple quantum order do not add destructively.[6] This corresponds to creating the negative of the Hamiltonian of equation 2 during the mixing period. Experimentally, applying a 90° phase shifted version of the preparation period pulses during the mixing period connects the Hamiltonian of equation 2 to its negative.

During the detection period, a pulsed spin locking sequence[10] of the form $(\pi/2)_x(-\theta_y)_n$ is used, resulting in a large increase in signal to noise over the detection scheme used earlier. The pulsed spin locking is not a

necessary component of the experiment, but is useful for signal enhancement in samples containing low ^1H concentrations. To obtain the maximum signal, the optimal value of θ is roughly 45° and the delay between pulses 40 μsec. One point is sampled after the first pulse and after each θ_y pulse: usually 512 or 768 spin locked points were acquired, subject to the constraints of the $T_{1\rho}$'s of the material. All these points are then averaged together to give a final point for a particular value of t_1. The entire sequence is repeated for different values of t_1 to obtain the multiple quantum free induction decay. Fourier transformation with respect to t_1 then yields the multiple quantum spectrum for a particular preparation time.

Experiments were performed on a homebuilt spectrometer operating at a ^1H Larmor frequency of 180 Mhz. The spectrometer was equipped with quadrature phase genaration circuits that produce rf pulses with relative phases of 0°, 90°, 180° and 270° at 30 Mhz intermediate frequency. Additional phase shifts needed for TPPI were performed by a digitally controlled phase shifter, in series with the quadrature generation, capable of 1.4° phase increments. For most spectra, obtaining ± 16 multple-quantum orders was sufficient. The orders were accomodated by incrementing the phases of the preparation period pulses by 11.25° for each t_1 value. The total bandwidth was 2.5 Mhz, resulting in a separation between orders of 78.125 kHz. The basic cycle time was 60 μsec with delays Δ = 2.5 μsec and Δ'= 7.5 μsec. The pulse length t_p was equal to 2.5 μsec.

Results and Discussion

Measurement of cluster sizes. The number of correlated spins at a particular preparation time dictates the intensity distribution of the

signal over the multiple quantum orders. For a finite cluster of size N, ignoring symmetry, the integrated spectral intensity per order can be related to the number of multiple-quantum transitions within that order.[11] These can be calculated directly from combinatorial arguments; for example the number of $n = \Delta M$ quantum transition in an N spin system is:[12]

$$\binom{2N}{N-\Delta M} = 2N!/(N - \Delta M)!(N + \Delta M)!$$

which can be approximated by a gaussian distribution for large N and $n << N$. As a result, the integrated multiple-quantum intensities fall off in a gaussian manner, $I(n) \sim \exp(-n^2/N)$, and are dictated by the size of the system.

The simplest assumption for a solid, which consists essentially of an infinite number of spins, is to subdivide the infinite spin system into finite spin systems which grow in the time-dependent fashion already portrayed by figure 3. Then we can represent the number of spins that have become correlated for a preparation time τ by an effective system size $N(\tau)$.[2] This time-dependent parameter is calculated as shown in figure 5, by fitting the integrated intensities to a gaussian and associating the standard deviation, σ, of the gaussian with $(N/2)^{1/2}$. The pattern and rate of growth of $N(\tau)$ over time will reflect the distribution of atoms in the sample. In the following sections the time dependent behavior of isolated clusters, concentrations of clusters and uniform distributions will be examined from this point of view.

Isolated clusters: Liquid crystal. In a nematic liquid crystal sample, owing to rapid translational diffusion, intermolecular dipolar couplings are averaged to zero while intramolecular couplings remain large.[13] The nematic

phase of the 21 spin p-heptyl-p'-cyanobiphenyl (molecular formula shown in figure 6) liquid crystal sample was thus selected to demonstrate an "ideal" case of isolated clusters on the NMR timescale, in the sense that individual molecules behave like solid clusters while still being completely independent of one another. Thus, this liquid crystal which contains 21 protons should be a good model for a 21 spin cluster. Figure 6 shows a plot of the n-quantum intensity normalized to the total intensity, versus preparation time; at short times, the number of multiple quantum orders increases, whereas for times greater than 1000 μsec the number of orders and their relative intensities remain unchanged. Reflecting the trends of the multiple quantum intensity plot, the effective system size $N(\tau)$, plotted in figure 6, grows for times up to 1000 μsec, after which it remains completely constant with a value of 21. The effective system size does not grow beyond the actual size of the molecule confirming that intermolecular couplings are zero and that only spins within the molecule can become correlated with one another. This type of behavior, the levelling of $N(\tau)$, is characteristic of isolated clusters.

Concentration effects: 1,8-dimethylnaphtalene-d_6. Solid solutions of six spin clusters were prepared to examine the effects of different degrees of cluster concentrations on the multiple quantum dynamics. The six spin clusters are formed by intimately mixing 1,8-dimethylnaphtalene-d_6 (DMN-d_6) with perdeuterated DMN-d_{12}; three concentration levels, 5, 10 and 20 mole %H were prepared in addition to the neat material. For the latter, the shortest intermolecular ^1H-^1H distance is 2.0 A along the b axis and the intramolecular methyl groups are sparated by 2.93 A. The unit cell is arranged such that the methyl groups of a pair of molecules are pointing

toward one another.[14] Dilution of the protonated DMN-d_6 in a perdeuterated lattice forces the inter-cluster distances to increase without affecting the intra-cluster distances. Therefore, relative differences in the development of multiple quantum intensities can be attributed to inter-cluster correlations.

Figure 7 shows plots of the integrated n-quantum intensity to the total intensity for these four samples of DMN, versus preparation time. Clearly, the trend indicates a more rapid development of multiple quantum orders as the concentration of the clusters is raised. In the 5 mole % solution, after an initial induction period, the number of orders remains fixed up to roughly 500 μsec, after which the intensites begin to grow slowly. By contrast, the 10 and 20 mole % solutions show orders growing in slowly all the time. Qualitatively, the features and ultimate intensities of the 10 and 20 mole % samples appear very similar, differing predominantly in the time scale of development. The multiple quantum intensities in the neat material increase very rapidly.

Plots of $N(\tau)$ versus τ are drawn for the 100, 20, 10 and 5 mole % solutions of DMN-d_6, in figure 8. The values of $N(\tau)$ are represented by the smooth solid line. Two extreme behaviors are illustrated in this figure: in the 5 mole % solution, $N(\tau)$ grows very little up to 500 μsec and then begins to increase slowly at longer times, whereas in neat DMN-d_6, $N(\tau)$ increases very rapidly. In the first case, the concentration of clusters is dilute enough to localize the interacting spins to the clusters only, for the duration of 500 μsec; in the second case, the unbounded spin system allows an increasing number of atoms to interact with one another, over time, in a monotonic fashion. In neat DMN-d_6, even though the ring positions are deuterated, the density of spins is high enough and the inter

and intra-molecular couplings comparable enough to blur the distinction between a clustered distribution and a uniform environment of hydrogen atoms. In the intermediate cases of 10 and 20 mole % solutions, where the concentration of clusters is raised, but where well-defined groups still exist, $N(\tau)$ grows continuously although more slowly than for neat DMN. On the time scale of the experiment, spins from different groups are close enough together to influence the multiple quantum dynamics to the point where inter-cluster separations are too small to produce a discernible plateau in $N(\tau)$ versus τ. Higher cluster concentration levels result in more rapid inter-cluster communication, as demonstrated by the steeper growth of $N(\tau)$ for the 20 versus the 10 mole % solution.

Two-Gaussian model. In the intermediate cases, where clusters exist but are not sufficiently isolated to preclude small interactions between them, a second time dependent parameter is introduced to ascribe a size to the clusters independently of inter-cluster events. A schematic drawing of a two Gaussian model is presented in figure 9. The simplest approximation is to attribute the multiple quantum intensities to two independent events: the intra-cluster correlations which have already matured, and the inter-cluster correlations that continue to develop between spins of different groups. The multiple quantum intensities due to the subgroup of clustered spins is approximated by a Gaussian whose variance is associated with $N_c/2$, while the remaining intensity is approximated by a second Gaussian of variance $N_2/2$. The total intensity is the sum of both contributions and is written as:

$$I(n)=m_c e^{-n^2/N_c} + m_2 e^{-n^2/N_2} \quad .$$

Only when the correlations due to clusters dominate the multiple quantum intensities, or when $m_c > m_2$, can the inter versus intra-cluster interactions be addressed separately to obtain N_c. A least squares iterative program using the Newton-Raphson method was employed to fit the multiple quantum intensities to the above equation. Now the two-time dependent parameters which will be considered are $N_c(\tau)$, the cluster size obtained from the two-Gaussian model and $N(\tau)$, obtained by fitting the integrated intensities to a single Gaussian as before. The pattern of growth of both parameters is used to establish the size and extent of clustering in solid samples. In the same spirit as for $N(\tau)$, absence of change in $N_c(\tau)$ over time is evidence that clusters exist, although they may be near one another. The magnitudes of m_c, m_2 and N_2 change to account for the increasing number of communicating clusters over time until finally m_2 becomes larger than m_c and the approximation is no longer valid.

Returning to figure 8, the values of $N_c(\tau)$ for the 4 concentrations of DMN are now plotted along with the values of $N(\tau)$ discussed earlier. Considering the two extremes once again, we note that $N_c(\tau)$ is not necessary to determine the cluster size in the 5 mole % solution, as here $N(\tau)$ remains fixed for a sizeable duration of time. $N_c(\tau)$ can be calculated at longer times and results in values close to six. By contrast, $N_c(\tau)$ and $N(\tau)$ both increase in the 100 % DMN sample, confirming that the density of spins is too high to assign a cluster size to this material. For the intermediate concentrations of 10 and 20 mole % where $N(\tau)$ grew uninterruptedly, $N_c(\tau)$ now remains constant over time with values about six. These data show what we should expect in a case like DMN containing predominantly clusters of six atoms which become increasingly close to one another as the ^1H concentration is raised.

1,8-dimethylnaphtalene-d_{10}. 1,8-dimethylnaphtalene-d_{10} (DMN-d_{10}) is very similar to 1,8-DMN-d_6, but here, in addition to ring deuteration, the methyl groups are partially deuterated as well leaving only two hydrogen atoms on the entire molecule. The inter and intra-molecular ^1H- ^1H distances are not affected by the additional methyl deuteration. Two solid solutions of DMN-d_{10}, 5 and 10 mole %, were prepared in the same manner as those of DMN-d_6. Plots of the integrated n-quantum intensities appear in the upper portions of figures 10a and 10b. In the 5 mole % solution, where the 2-quantum intensity is essentially dominant at all times, the effective system size, $N(\tau)$, is calculated directly from the binomial formula of equation 2. For the 10 mole % solution, the combinatorial formula is used up to 600 μsec, after which the intensities can be approximated by a Gaussian as usual.

A comparison of the six spin and two spin model clusters at comparable ^1H concentrations reveals similar trends for $N(\tau)$ and $N_c(\tau)$; in both 5 % cases, $N(\tau)$ remains level up to approximately 500 μsec after which it increases slowly, whereas in the 10 % cases $N(\tau)$ rises more steeply. What distinguishes the two materials from one another are the actual values of the effective system and cluster sizes. In DMN-d_{10}, contrary to DMN-d_6, $N(\tau)$ remains close to two; in the 10 % solution, $N_c(\tau)$ can be calculated at long times and lies between three and four. These results demonstrate that the multiple quantum dynamics are sensitive enough to distinguish clearly between two spin and six spin clusters of very similar compounds.

Hexamethylbenzene. Protonated molecules of hexamethylbenzene are mixed with perdeuterated molecules to create clusters of 18 atoms. Two molecular motions exist in HMB at room temperature: each methyl group reorients about

its C_3 axis, and the entire molecule undergoes fast limit sixfold hopping about the C_6 axis of the benzene ring.[15] In neat HMB, C-C distances between molecules range upwards from 3.7 Å; average distances between protons on different methyl groups range from 3.3Å to 6.6 Å.[16] Five mole % solutions were prepared and values of $N(\tau)$ and $N_c(\tau)$ are plotted in figure 11. From the trends in $N(\tau)$ it is clear that the cluster concentration is too high to resolve the individual cluster size. On the other hand, the values of $N_c(\tau)$ remain constant, over time, at roughly 15, indicating that fairly large clusters exist in the dilute sample.

1,2,3,4-tetrachloronaphtalene-bis(hexachlorocyclopentadiene)-adduct. This polycrystalline sample encompasses the characteristcs of a clustered material as well as a neat sample. On the one hand, the bulky hexachlorocyclopentadiene groups isolate hydrogen atoms of different molecules from one another, creating a sharp variation of inter versus intra-molecular dipolar coupling strenghts: on the other hand, the "cluster concentration", or cluster to solvent-atom ratio, is high. No crystal structure is available for this material. The ^1H NMR spectrum is very broad, on the order 50 kHz, and structureless. A zero field NMR spectrum was obtained and computer simulations were performed to determine the positions of the 4 hydrogen atoms. With an assumed C_2 axis of symmetry, only four distances are needed to characterize the hydrogen spectrum: r_{11}=2.83 Å, r_{12}=2.22 Å, $r_{12'}$= 4.34 Å, and r_{22}= 5.01 Å.[17]

The integrated multiple quantum intensities in figure 12a show a discontinuity in the development of the multiple quantum coherence. Up to 300 μsec, only two and a small amount of four quantum coherence have grown; thereafter, many high orders appear rapidly. It is interesting to note the

difference between the time development of these intensities relative to those of the liquid crystal sample shown in figure 6. The plot of $N(\tau)$ versus τ in figure 12b reflects the trends of the multiple quantum intensities; the effective size of the system remains at four for times ranging up to 300 μsec and then shoots up rather rapidly. From these trends it is clear that correlations develop very quickly for hydrogen atoms within the molecule; at longer times, the smaller dipole couplings become more important and communication occurs between spins on different molecules as well. Because $N_c(\tau)$ and $N(\tau)$ both increase at longer times, this sample appears to have similar properties to the neat DMN sample shown in Figure 8d. Perhaps it can be best thought of as a borderline case where the cluster size can be determined from the plateau in $N(\tau)$ at short times.

Hydrogenated Amorphous Silicon. A critical level of hydrogen incorporation into amorphous silicon thin films modifies their electrical properties and allows them to be used as semiconductors.[1] By characterizing the hydrogen distribution in the thin films, insight concerning the relationship between the structure of hydrogenated amorphous silicon (a-Si:H) and its properties can be gained. To motivate some of the important questions, a hypothetical drawing of local hydrogen structure is presented in figure 13. The ^1H NMR spectrum of hydrogenated amorphous silicon can be decomposed into two resonance lines: one narrow (3-4 kHz) and one broad (25 kHz).[18] The 4 atom % H contributing to the narrow component is present as spatially isolated monohydrides and molecular H_2. The remaining hydrogen, which consists of between 4 and 16 atom % H in device quality films, is attributed to clusters of monohydrides.

We have used multiple-quantum NMR to determine the size and extent of

clustering in a-Si:H thin films.[3] Shown in figure 14 are plots of the number of correlated spins versus time for a number of samples containing different concentrations of hydrogen. In figure 14a, two extremes are presented: a 50 atom % sample for which the effective system size grows rapidly and continuously and an 8 atom % sample for which $N(\tau)$ remains essentially constant over time. The trends in these plots indicate that the polymeric sample consists of a continuous network of atoms, whereas the 8 atom % sample is composed of clusters of approximately six atoms. A plot of the number of correlated spins for an a-Si:H sample containing 16 atom % H is shown in figure 14b: values of $N(\tau)$ increase over time, whereas $N_c(\tau)$ levels off at six. Similarly to the 8 atom % sample, the size of the clusters in the 16 atom % sample is approximately six, but now they exist in higher concentrations, as evidenced by the more rapid growth of $N(\tau)$. The values in these plots are very similar to those of 1,8 DMN in perdeuterated DMN shown in figure 8.

Summary

Multiple quantum NMR, a technique which induces spins to act collectively through their dipolar couplings, is used to determine the spatial distribution of atoms in materials lacking long-range order; in particular, the size and extent of clustering is probed. Based on the proximity of spins to one another, correlations between them will develop more or less rapidly. A time-resolved multiple quantum experiment measures both the number of correlated spins and the rate at which these develop. The key feature in the time-dependent experiments is that in clustered materials, where groups are physically isolated from one another, the number

of absorbed quanta and correlated spins is essentially bounded, on the experimental time scale, by the size of the cluster. In a uniform distribution, however, the interacting network of spins increases monotonically with time. These events are displayed in the multiple quantum spectra by changes in the overall intensity distribution across the multiple quantum orders. The intensity envelope is quantified by two time-dependent parameters, the effective system size $N(\tau)$ and the effective cluster size $N_c(\tau)$. Thus by studying the trends in $N(\tau)$ and $N_c(\tau)$, i.e. whether they level off or grow with time, we can ascertain the size and extent of clustering in solids.

Model systems containing different hydrogen environments were investigated by this technique: a liquid crystal in which inter-cluster couplings were zero; solid solutions consisting of protonated samples mixed with perdeuterated counterparts in which inter-cluster distances were varied by manipulating the level of dilution; neat protonated polycrystalline solids where inter and intra-cluster dipolar couplings were roughly comparable and hydrogenated amorphous silicon thin films containing different concentrations of hydrogen atoms. The atomic distributions in these materials ranged from truly isolated clusters to uniformly distributed arrangements, with emphasis on the intermediate cases where concentrations of clusters were addressed. These techniques are presently being used to study clustering of molecules adsorbed on zeolites and trapped in silicate glasses.

ACKNOWLEDGEMENTS

We gratefully acknowledge helpful discussions and assistance from Dr. M. Munowitz, Dr. A.N. Garroway, Prof. J. Reimer and Karen Gleason throughout the course of this work. This work was supported by the Director, Office of Energy Research, Office of Basic Energy Sciences, Materials Sciences Divsion of the U.S. Department of Energy and by the Director's Program Development Funds of the Lawrence Berkeley Laboratory under Contract No. DE-AC03-76SF00098.

References

1. Semiconductors and Semimetals, Hydrogenated Amorphous Silicon, Volume 21, edited by J.I. Pancove (Academic Press, Orlando, 1984).

2. Baum, J.; Munowitz, M.; Garroway, A.N.; Pines, A. J. Chem. Phys. **83**, 2015-2025 (1985).

3. Baum, J.; Gleason, K.K.; Pines, A.; Garroway, A.N.; Reimer, J.A. submitted to Phys. Rev. Lett.

4. Wang, P.K.; Slichter, C.P.; Sinfelt, J.H. Phys. Rev. Lett. **53**, 82 (1984).

5. a) Bodenhausen, G. Prog. NMR Spectrosc. **14**, 137 (1981); b) Weitekamp, D.P. Adv. Magn. Reson. **11**, 111 (1983); c) Munowitz, M; Pines, A. Adv. Chem. Phys., in press.

6. Yen, Y.S.; Pines, A. J. Chem. Phys. **78**, 3579 (1983).

7. Aue, W.P.; Bartholdi, E.; Ernst, R.R. J. Chem. Phys. **64**, 2229 (1976).

8. Warren, W.S.; Weitekamp, D.P.; Pines, A. J. Chem. Phys. **73**, 2084 (1980).

9. a) Drobny, G.; Pines, A.; Sinton, S.; Weitekamp, D.P.; Wemmer, D. Faraday Symp. Chem. Soc. **13**, 49 (1979); b) Bodenhausen, G.; Vold, R.L.; Vold, R.R. J. Magn. Reson. **37**, 93 (1980).

10. a) Ostroff, E.D.; Waugh, J.S. Phys. Rev. Lett. **16**, 1097 (1966); b) Rhim, W.-K.; Burum, D.P.; Elleman, D.D. Phys. Rev. Lett. **37**, 1764 (1976); c) Suwelack, D.; Waugh, J.S. Phys. Rev. **B22**, 5110 (1980); d) Maricq, M.M. Phys. Rev. **B25**, 6622 (1982).

11. Murdoch, J.B.; Warren, W.S.; Weitekamp, D.P.; Pines, A. J. Magn. Reson. **60**, 205 (1984).

12. a) Wokaun, A.; Ernst, R.R. Mol. Phys. **36**, 317 (1978); b) Hoffman, R.A Adv. Magn. Reson. **4**, 87 (1970).

13. De Gennes, P.G. The Physics of Liquid Crystals (Clarendon Press, Oxford, 1974).

14. Bright, D.; Maxwell, I.E.; de Boer, J. J. Chem. Soc. Perkin Trans. **II**, 2101 (1973).

15. a) Andrew, E.R. J. Chem. Phys. **18**, 607 (1950); b) Wemmer, D.E.; Ph.D. thesis, University of California, Berkeley, 1978, pp. 38-43 (published as Lawrence Berkeley Laboratory Report LBL-16119).

16. Wyckoff, R.W.C. Crystal Structures (Interscience New York, 1966), Vol. 6, Part 1, p. 386.

17. Zax, D.B.; Bielecki, A.; Zilm, K.W.; Pines, A.; Weitekamp, D.P. J. Chem. Phys. 83, 4877 (1985).

18. a) Taylor, P.C. Semiconductors and Semimetals, Hydrogenated Amorphous Silicon, Volume 21, Part C., pg. 99; b) Reimer, J.A.; Vaughan, R.W.; Knights, J.C. Phys. Rev. Lett. 44, 193 (1980).

Figure Captions

Figure 1

Possible atomic distributions in solids. Uniform and clustered distributions can be distinguished by time-resolved solid-state multiple-quantum NMR.

Figure 2

180 Mhz ^{1}H multiple-quantum NMR spectra of the polycrystalline sample 1,2,3,4-tetrachloronaphtalene-bis(hexachlorocyclopentadiene)-adduct. The time development of the multiple-quantum coherences is discontinuous in this clustered material. The spectra change very little over the first 300 μsec, indicating a limited spin system on this time scale. At longer times, when intermolecular interactions develop, the system is no longer bounded and higher multiple-quantum orders arise in the spectrum.

Figure 3

In multiple quantum NMR, spins, symbolically represented here by hatched circles, become correlated with one another over time, through pairwise dipolar interactions: the closer the spins, the shorter the time needed for interactions to develop. For uniformly distributed spins (a), correlations will be expected to develop monotonically with time. In a clustered material (b), however, the magnitudes of the inter versus intra-cluster dipolar couplings are quite different. At short times, the number of correlated spins will be limited to the number of atoms in the cluster whereas at long times intercluster interactions will develop and all the spins will

become correlated with one another. The difference between clustered and uniform distributions is observable in the time-dependence of the n-quantum absoprtion a seen in Figure 2.

Figure 4

Two-dimensional multiple-quantum pulse sequence for solids. The preparation and mixing periods are composed of 8 $\pi/2$ pulses of length t_p(=2.5 μsec) separated by delays Δ(=2.5 μsec) and Δ'(=7.5 μsec). The total preparation/mixing time τ is achieved by repeating the basic 60 μsec cycle m times. When the phases of the pulses are x and $\bar{x}$, the Hamiltonian is equal to 1/3 $(H_{yy} - H_{xx})$; during the mixing period, when the phases of the pulses are y and $\bar{y}$, the Hamiltonian becomes $-1/3\ (H_{yy} - H_{xx})$, i.e. the negative of the preparation period Hamiltonian. To separate the multiple-quantum orders, the preparation period pulses are incremented by a phase ϕ for each value of t_1. During the detection period, a pulsed spin locking sequence is used for signal enhancement in samples containing low ^1H concentrations.

Figure 5

Top: 180 Mhz ^1H multiple quantum spectrum of the liquid crystal p-hexyl-p'-cyanobiphenyl in the nematic phase for a preparation time τ=660 μsec. Bottom: The data points are measured from the spectrum above by integrating each peak corresponding to each multiple quantum order. The resulting intensities are then fit to a gaussian distribution whose standard deviation, σ, is associated with $(N/2)^{1/2}$. The solid curve is the plot of the best fit value for N. N, the effective system size characterizes the number of correlated spins, in this case 20, at each preparation time.

Figure 6

a) n-quantum intensity versus preparation time for the liquid crystal p-hexyl-p' cyanobiphenyl in the nematic phase. The intensity of each multiple quantum order has been normalized to the total spectral intensity, and smooth curves have been drawn through the data points to aid the eye. From top to bottom, n=2 corresponds to open circles; n=4 to filled circles; n=6 to open squares; n=8 to closed squares; n=10 to open triangles. After roughly 1000 μsec, no new multiple quantum orders develop and their relative intensities remain unchanged.

b) $N(\tau)$ versus τ for the liquid crystal sample. After an induction period, the effective system size $N(\tau)$ levels off at 21, indicating that the number of interacting spins is limited to the size of the individual liquid crystal molecules which contain 21 protons.

Figure 7

n-quantum intensity versus preparation time for solid solutions containing

a) neat 1,8-dimethylnaphtalene-d_6 (DMN-d_6).

b) 20 mole % solution of DMN-d_6 in 1,8-dimethylnaphtalene-d_{12} (DMN-d_{12}).

c) 10 mole % solution of DMN-d_6 in DMN-d_{12}.

d) 5 mole % solution of DMN-d_6 in DMN-d_{12}.

In all plots, the labelling of the multiple quantum orders are the same as for figure 6. The neat compound and the 5 mole % solution are examples of unlimited and clustered spin systems respectively. The 10 and 20 mole % samples are examples of more concentrated clustered environments. The general trend indicates that as the cluster concentration is lowered, the

multiple quantum intensity distribution changes less with time.

Figure 8

Number of correlated spins versus preparation time for the four solutions of DMN-d_6 described in figure 7. The filled circles represent values for $N(\tau)$, the effective system size, and the open ones values for $N_c(\tau)$, the effective cluster size. The size and extent of clustering can be determined from the pattern and rate of growth of $N(\tau)$ and $N_c(\tau)$.

a) both parameters grow uninterruptedly, indicating an unbounded spin system.

b) and c) In both samples, $N_c(\tau)$ remains constant over time, indicating clusters of six atoms; the more rapid growth of $N(\tau)$ in the 20 versus 10 mole % solution reflects the fact that the six spin clusters of DMN-d_6 become closer to one another as the ^1H concentration is raised.

d) After an initial induction period, $N(\tau)$ remains essentially constant up to approximately 500 μsec, indicating a bounded system of six atoms. At longer times when clusters interact, $N_c(\tau)$ remains level at six.

Figure 9

Schematic drawing of the two-Gaussian model. The inset represents clusters interacting with one another on the experimental time scale. In order to determine the cluster size, a parameter N_c is introduced to describe events occurring within a cluster, independently of those occurring between clusters. The multiple quantum intensities (filled circles) are the sum of intra and inter-cluster correlations both of which are associated, independently, with a Gaussian of standard deviation $(N_c/2)^{1/2}$ and $(N_2/2)^{1/2}$, re-

spectively. Only when most of the multiple quantum intensity is due to intra-cluster correlations is this approximation valid.

Figure 10

n-quantum intensity (top) and number of correlated spins (bottom) versus preparation time for two solid solutions:

a) 5 mole % 1,8-dimethylnaphtalene-d_{10} (diagrammed in the inset) in DMN-d_{12}.

b) 10 mole % DMN-d_{10} in DMN-d_{12}.

For the 5 mole % solution $N(\tau)$ remains close to 2. In the 10 mole % solution, $N(\tau)$ grows with time but $N_c(\tau)$ remains essentially constant hovering between 3 and 4. The cluster size in these samples is very small.

Figure 11

Number of correlated spins versus preparation time for hexamethylbenzene-h_{18} (shown in the inset) in hexamethylbenzene-d_{18}. In this 5 mole % solution, $N(\tau)$ grows steadily whereas $N_c(\tau)$ remains level at roughly 15 indicating fairly large clusters.

Figure 12

a) n-quantum intensity versus preparation time for the polycrystalline sample 1,2,3,4-tetrachoronaphtalene-bis(hexachlorocyclopentadiene)-adduct. The 2-quantum intensity is not plotted so that higher multiple-quantum orders can be seen more clearly. The time development of the multiple-quantum intensities is discontinuous.

b) Number of correlated spins versus preparation time for this sample. The effective system size $N(\tau)$ remains at 4 for times up to 300 μsec, indicating

that only the 4 hydrogen atoms within the molecule have become correlated thus far. At long times, a large number of intercluster interactions can develop.

Figure 13

Schematic 3-dimensional drawing of clustered monohydrides in hydrogenated amorphous silicon (a-Si:H). The silicon atoms are in a tetrahedral bonding configuration. Silicon atoms, hydrogen atoms and covalent bonds are represented by open circles, filled circles and solid lines, respectively. The drawing is intended to motivate questions concerning the distribution of hydrogen in a-Si:H thin film.

Figure 14

Number of correlated spins versus preparation time for:

a) 50 atom % and 8 atom % a-Si:H samples. For the 50 atom % sample, $N(\tau)$ grows very rapidly; whereas for the 8 atom % sample, $N(\tau)$ remains essentially constant at six.

b) 16 atom % a-Si:H sample. $N(\tau)$ remains nearly level up to 250 μsec, after which it increases slowly; $N_c(\tau)$ levels off at approximately six. Both the 16 and 8 atom % samples contain clusters of approximately six atoms; as the hydrogen level is raised, the cluster concentration is increased as well.

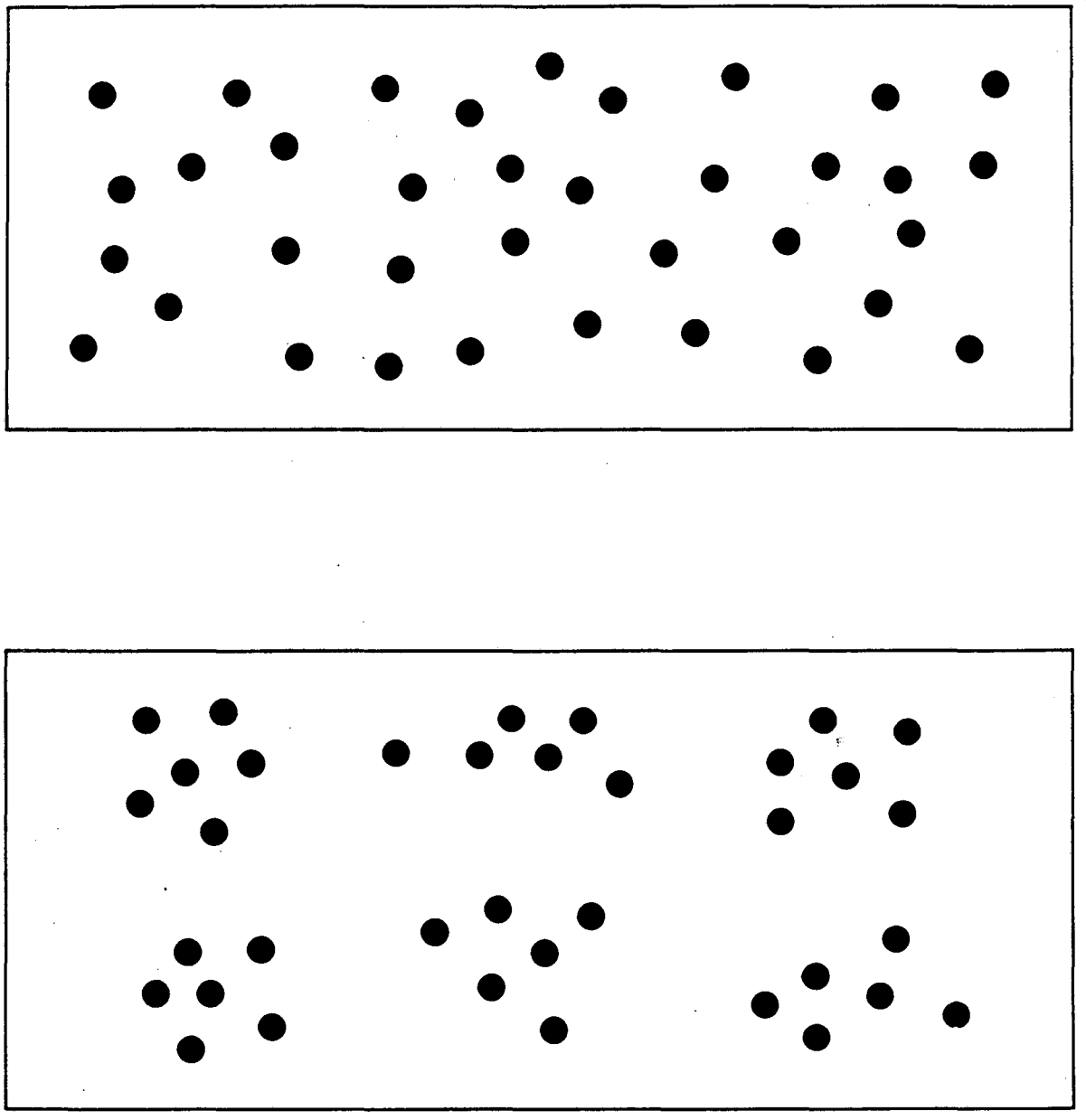

XBL 8511-12717

Figure 1

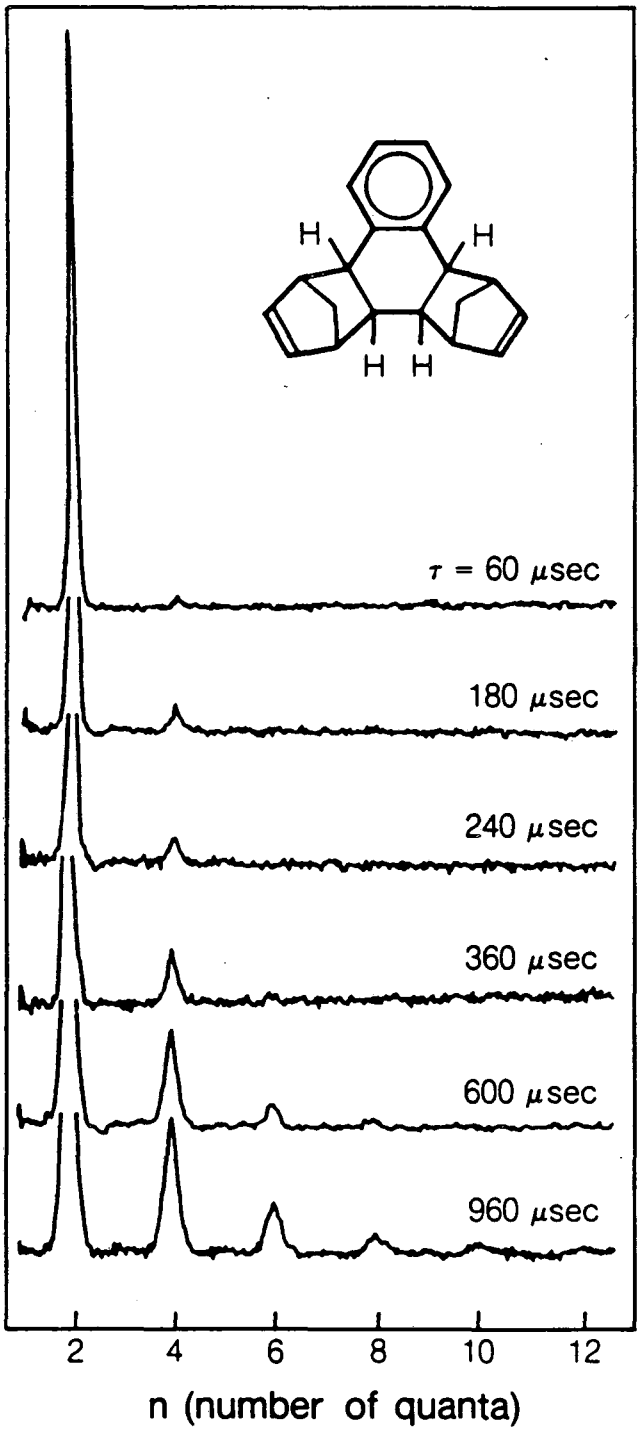

XBL 861-144
Figure 2

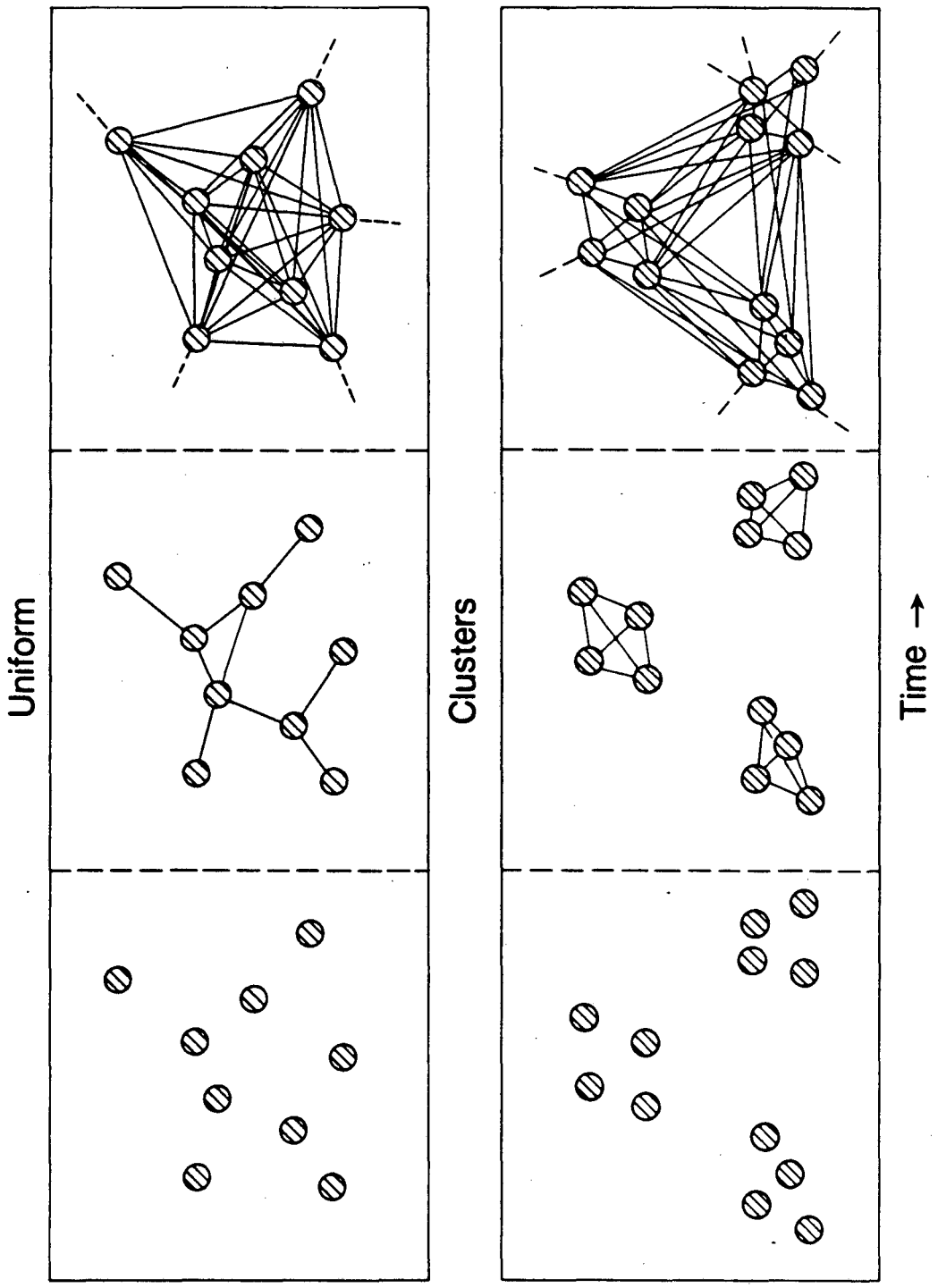

XBL 8511-12718 A

Figure 3

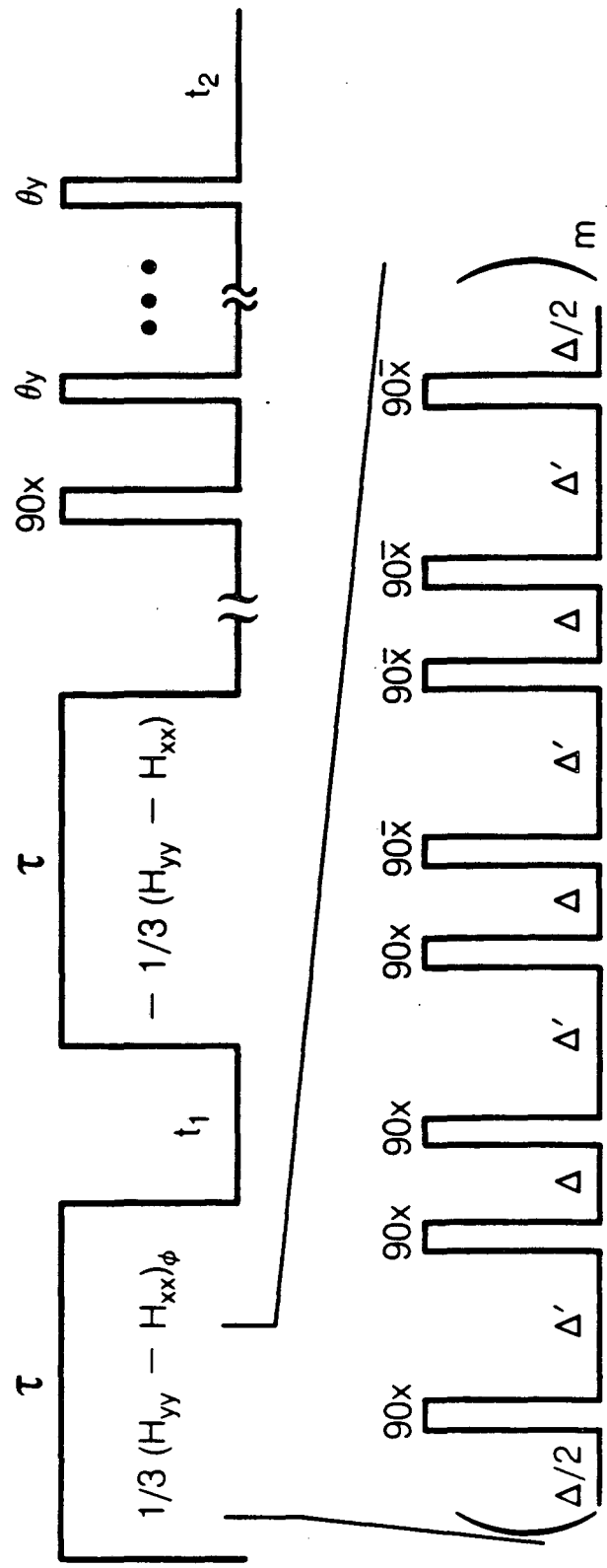

XBL 8512-5061

Figure 4

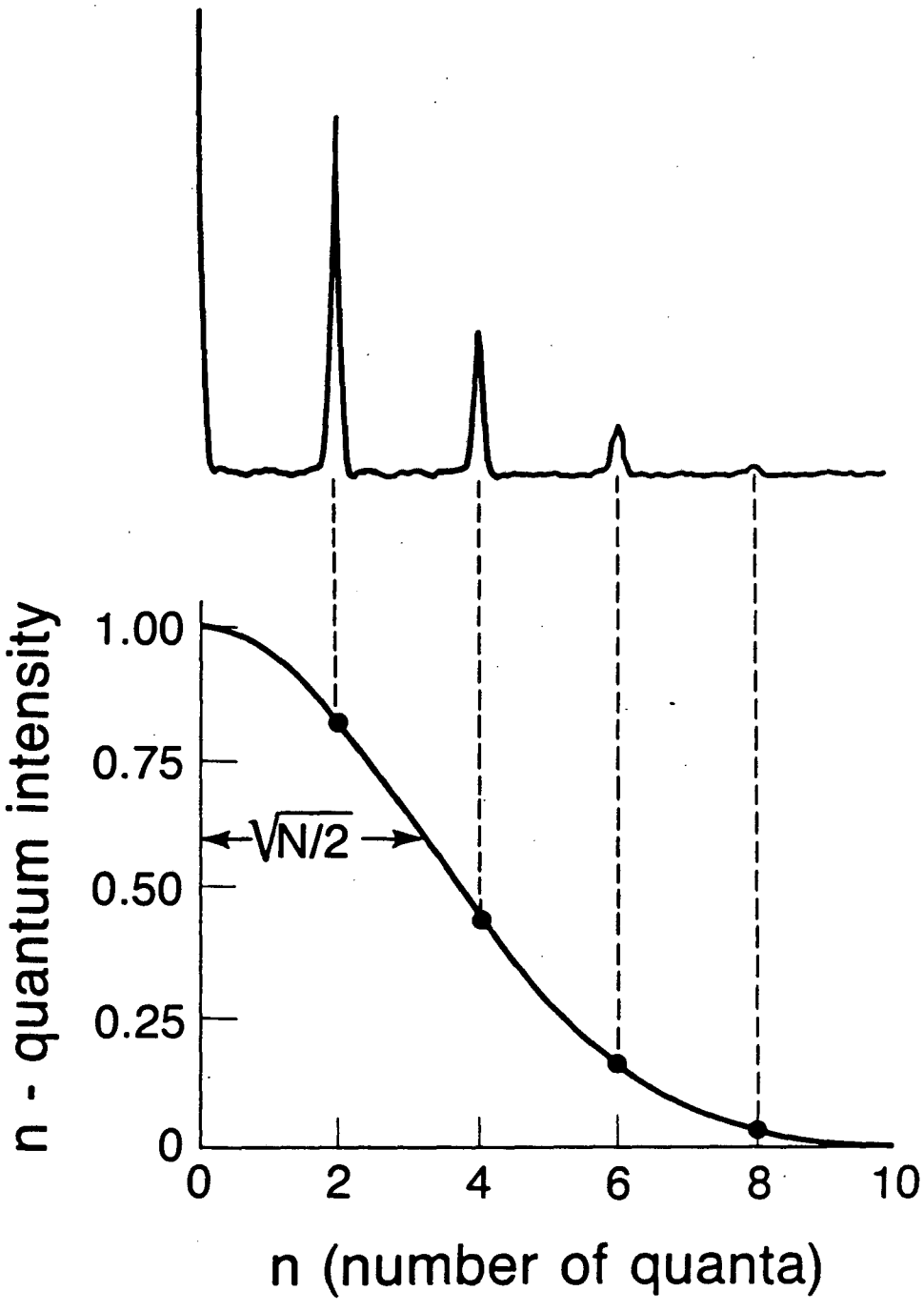

XBL 8511-12714
Figure 5

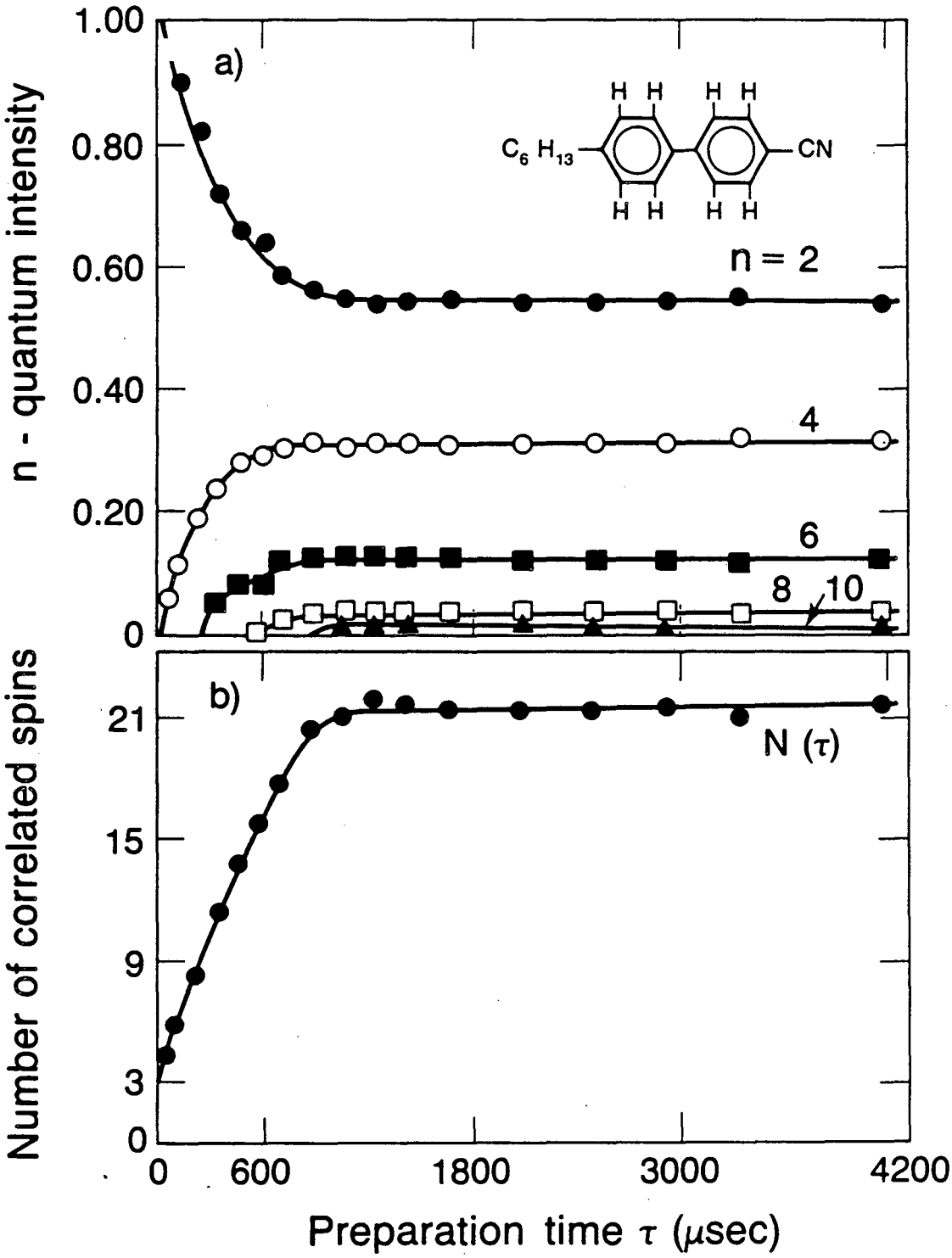

XBL 8512-12777

Figure 6

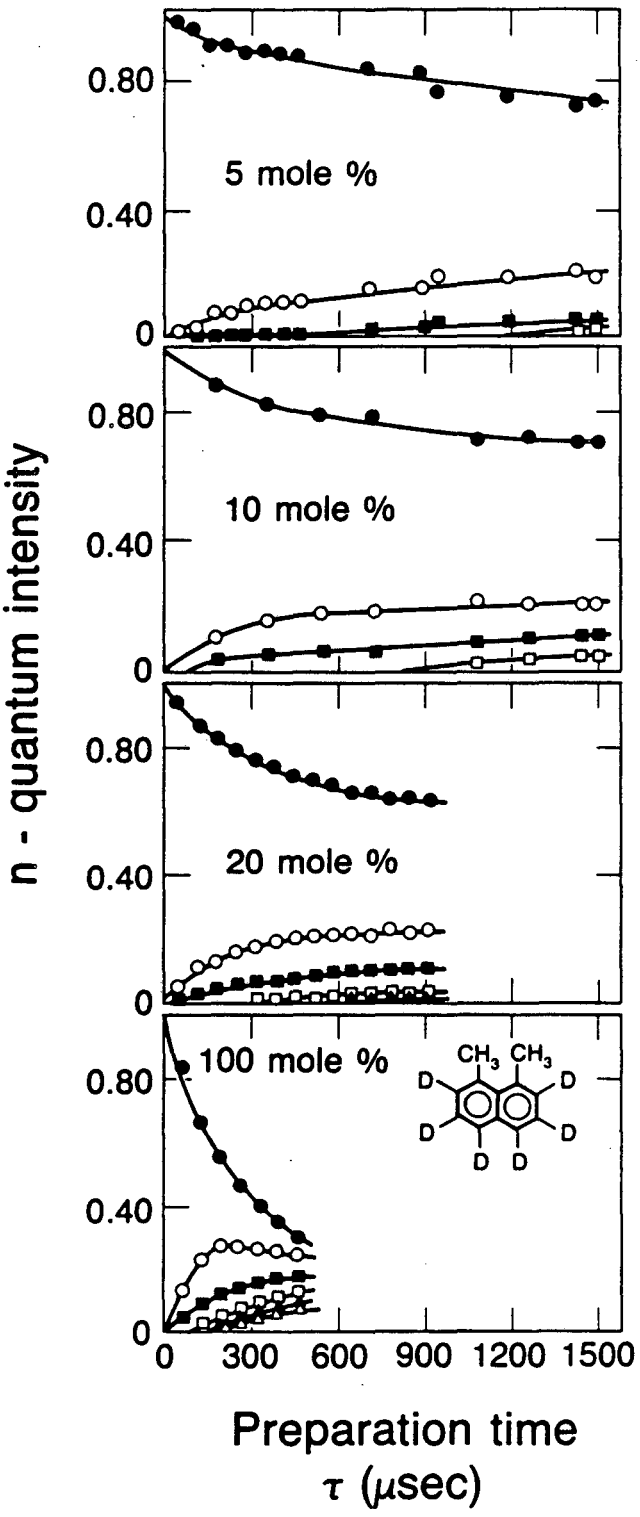

XBL 8512-12778

Figure 7

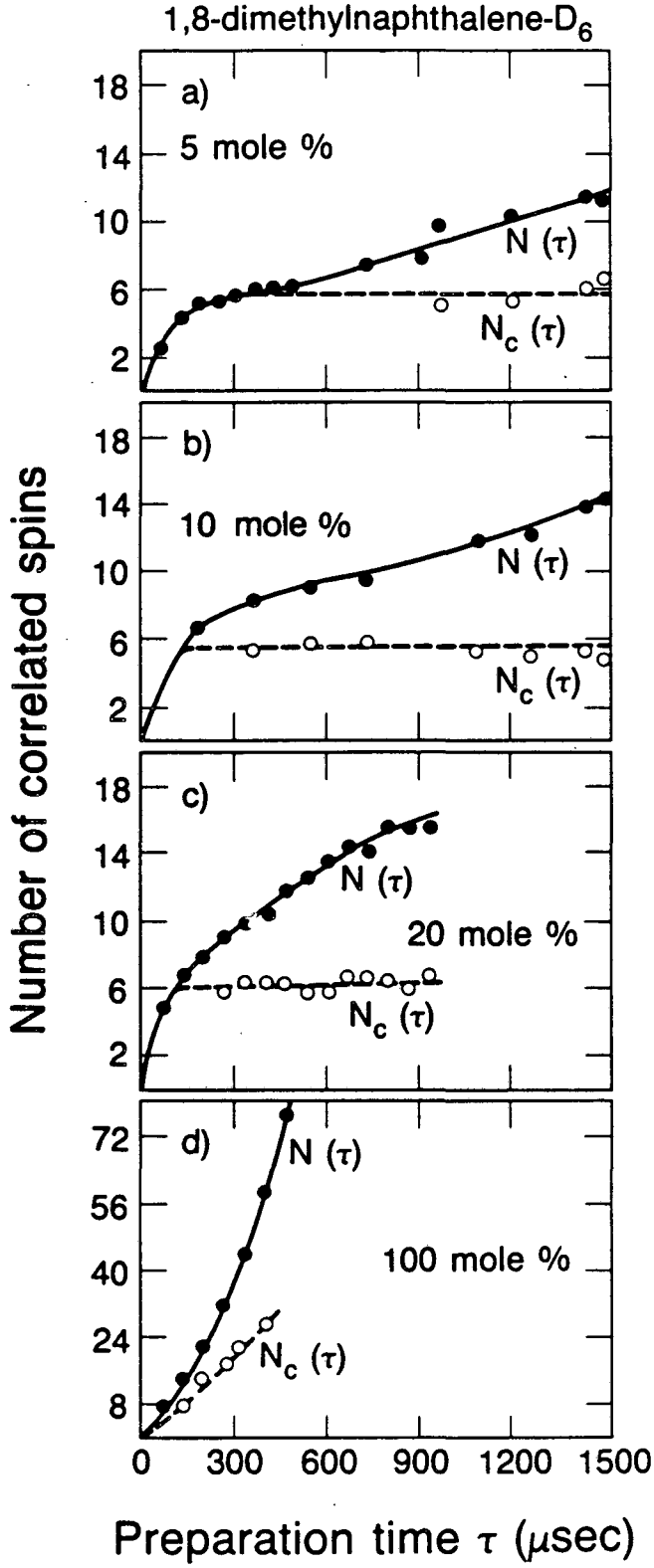

XBL 8512-12782

Figure 8

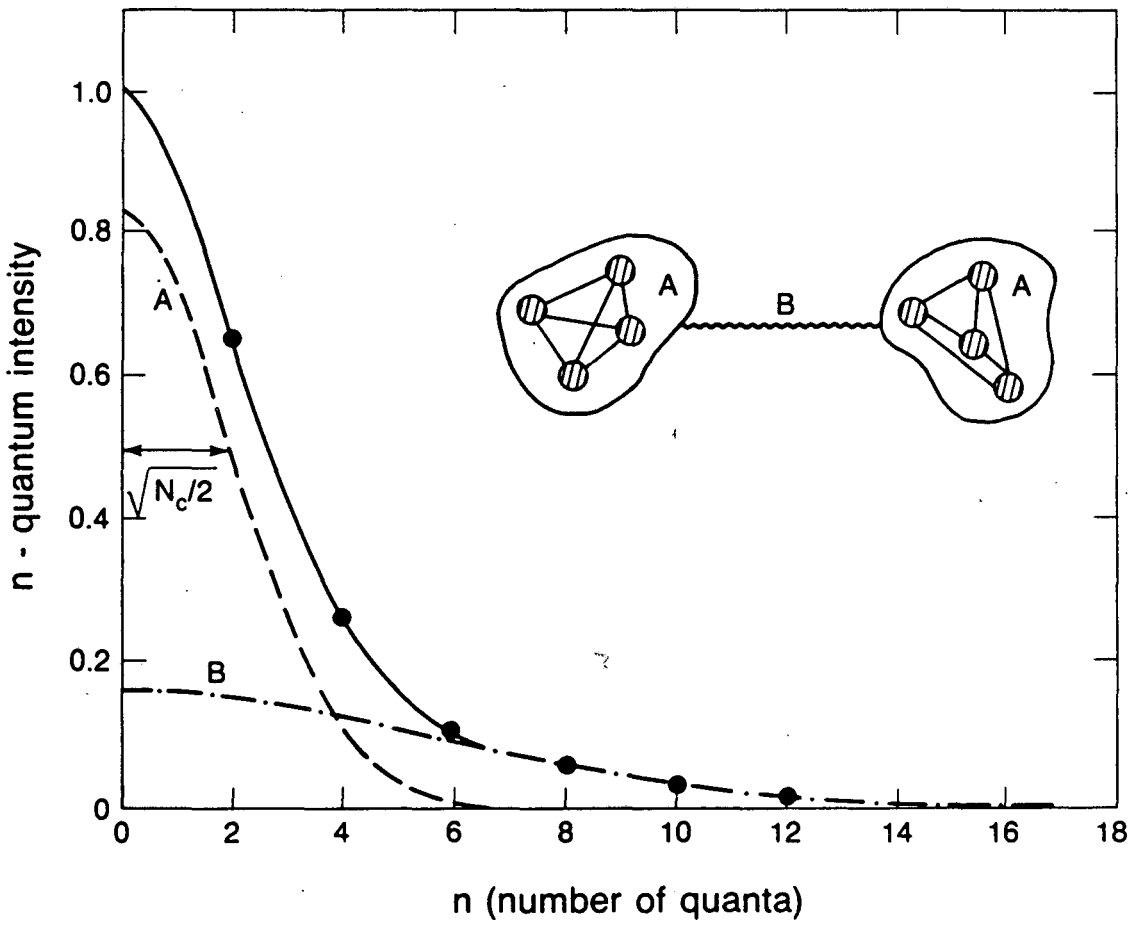

XBL 8511-12716

Figure 9

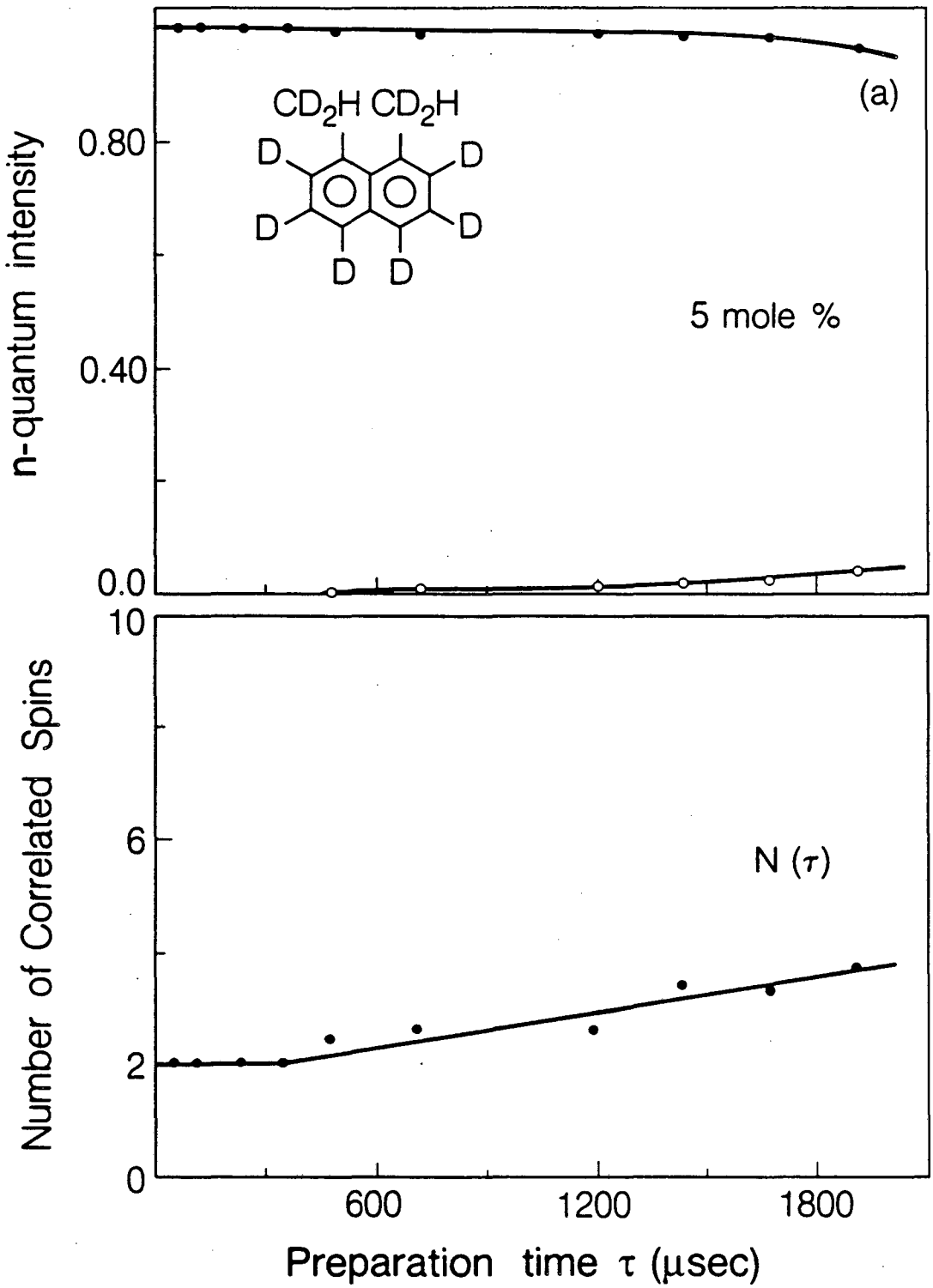

XBL 8512-5062
Figure 10a

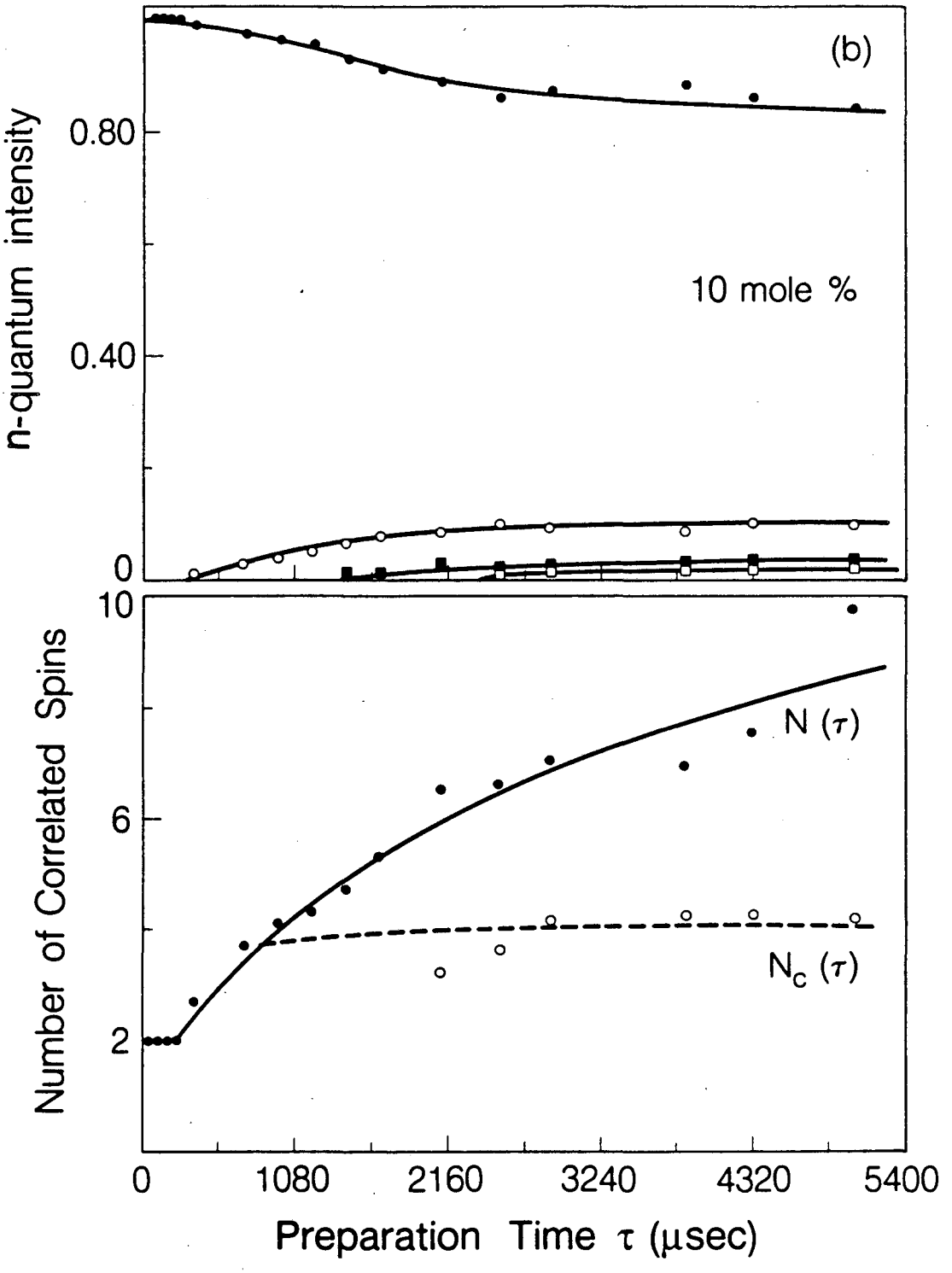

XBL 8512-5060

Figure 10b

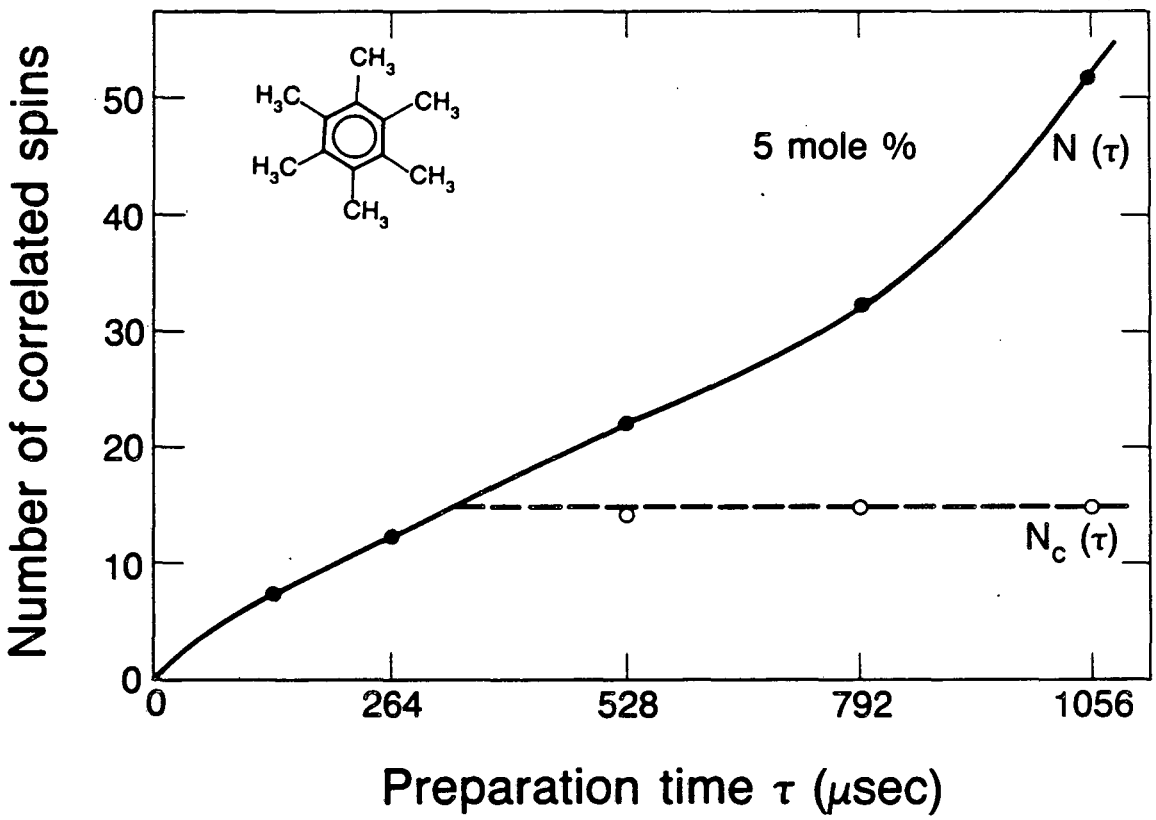

XBL 8512-12773

Figure 11

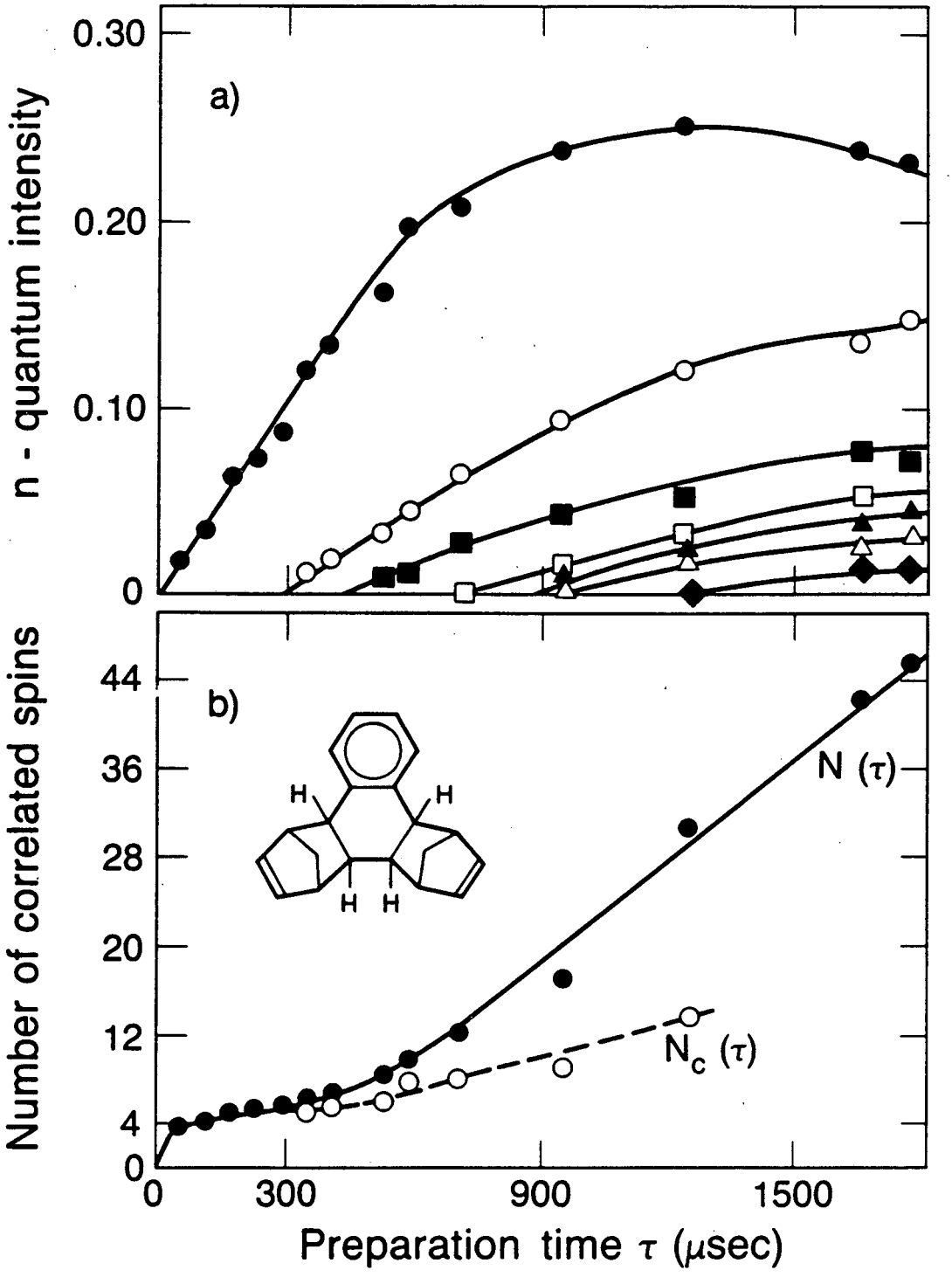

XBL 8512-12783

Figure 12

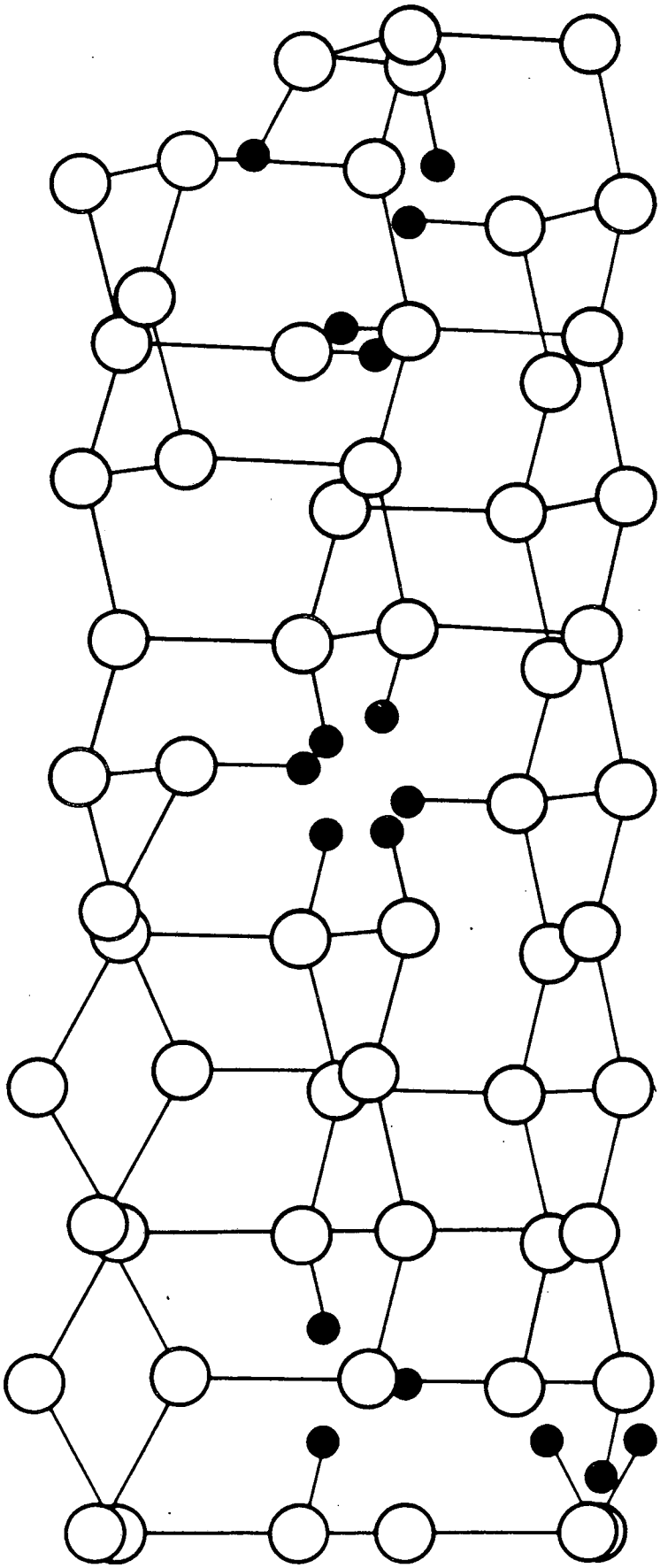

XBL 8510-4450

Figure 13

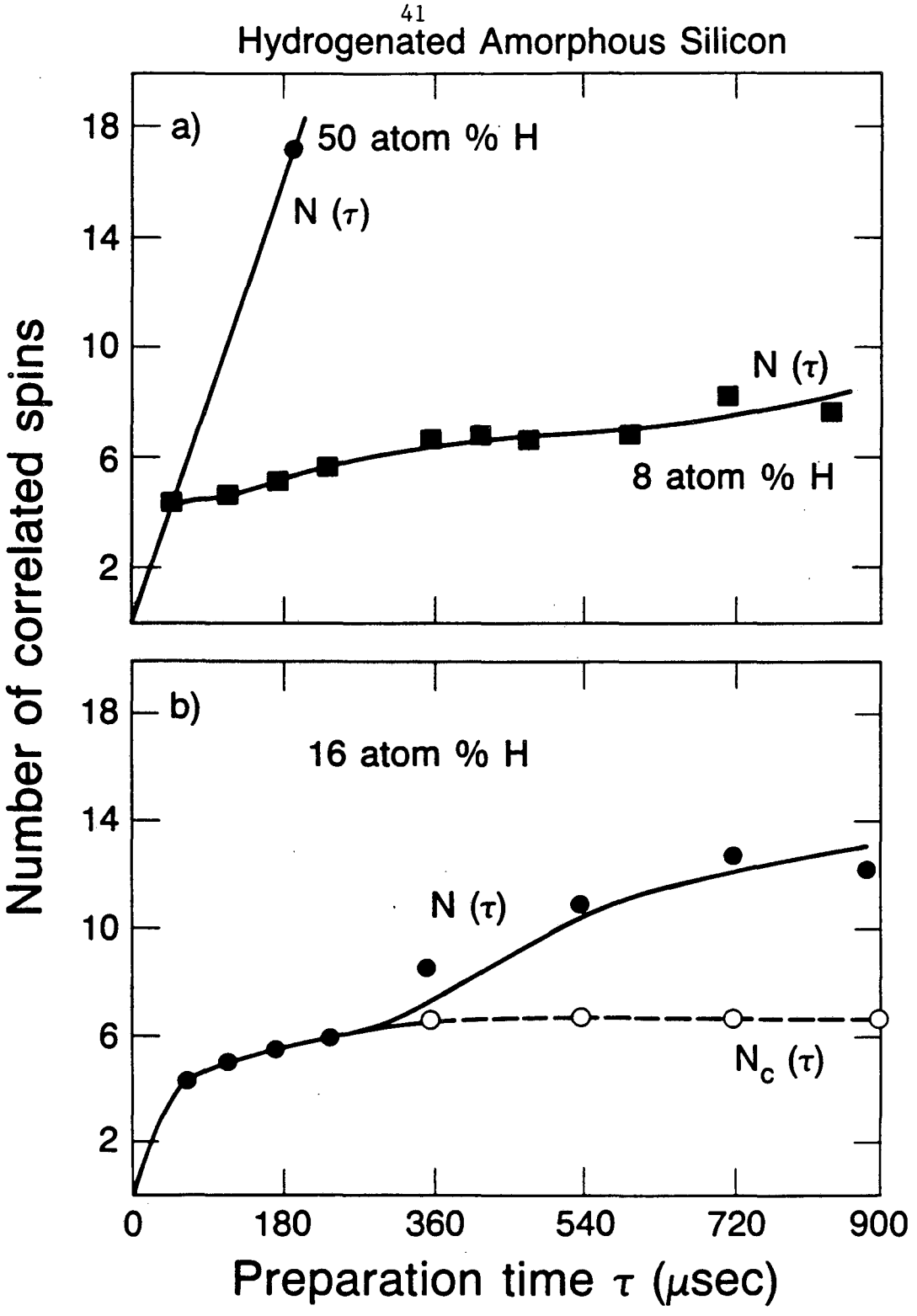

XBL 8512-12833

Figure 14

LAWRENCE BERKELEY LABORATORY
TECHNICAL INFORMATION DEPARTMENT
UNIVERSITY OF CALIFORNIA
BERKELEY, CALIFORNIA 94720